Research Square

Preprints are preliminary reports that have not undergone peer review.
They should not be considered conclusive, used to inform clinical practice,
or referenced by the media as validated information.

# Comparative Study on the Pathogenicity of Different Canine Distemper Virus Isolates in Mink

**Rongshan Tao**
Guizhou Medical University
**Dingfeng Long**
Guizhou Medical University
**Jianjun Zhao**
Heilongjiang Bayi Agricultural University
**Yu Cao**
2692327139@qq.com

Guizhou Medical University

**Research Article**

**Keywords:** Canine distemper virus, SDZC(17)M2, LNDL(17)M4, Hebei

**Posted Date:** October 16th, 2026

**DOI:** https://doi.org/10.21203/rs.3.rs-11102320/v1

**License:** This work is licensed under a Creative Commons Attribution 4.0 International License.
Read Full License

**Additional Declarations:** No competing interests reported.

## Abstract

# Objective

To establish a mink infection model and compare the pathogenicity and virulence of different CDV isolates.

# Methods

Three CDV strains, SDZC (17) M2, LNDL (17) M4 and Hebei, were intranasally inoculated into 60-day-old mink at $10^{4.0}$ $TCID_{50}$ for artificial infection and virulence assessment.

# Results

The three isolates induced clinical signs of varying severity and pathological lesions in multiple organs of mink. Mortality rates of SDZC(17)M2, Hebei and LNDL(17)M4 groups were 80%, 20% and 0%, with virulence/immunosuppression scores of 2/2.67, 1.1/2 and 0.85/1.73. The viruses replicated efficiently in target organs. SDZC(17)M2 reached viral loads up to $10^9$ copies/mL in lungs, lymph nodes and kidneys, significantly higher than the other two strains ($P < 0.05$). On day 14 post-infection, viral RNA in ocular, nasal and rectal swabs was also markedly elevated in SDZC (17) M2-infected mink ($P < 0.05$). TNF-α mRNA transcription was downregulated from 3 to 10 days post-infection and recovered at day 14, and was again downregulated at day 21. IFN-α and IFN-β transcription remained unchanged during 3–10 days post-infection but were upregulated on day 14, whereas IL-4 mRNA transcription was downregulated throughout 3–21 days post-infection.

# Conclusion

This study systematically characterized virulence and host immune responses of prevalent mink-origin CDV strains in China. SDZC (17) M2 is a highly pathogenic variant with strong shedding capacity and severe immunosuppression, potentially linked to H-protein receptor-binding mutations I542N and Y549H. These data support further mechanistic research and vaccine candidate screening for CDV.

## 1. Introduction

Canine distemper virus (CDV), an important member of the Morbillivirus genus within the Paramyxoviridae family, is a highly lethal pathogen capable of cross-host infection in a wide range of carnivorous animals, including Canidae, Mustelidae, and large Felidae species. It poses a persistent threat to the global fur-animal breeding industry and the conservation of endangered wild animals [1]. CDV is mainly transmitted via the oronasal route through aerosols and contaminated materials. After

infection, the virus initially targets the upper respiratory tract and tonsils, where it actively replicates in local dendritic cells, macrophages, and mononuclear cells of bronchial lymph nodes within 24 h, subsequently inducing viremia. In the late stage of infection, the virus extensively invades the gastrointestinal epithelium and central nervous system, resulting in severe catarrhal enteritis, bloody stool, and characteristic demyelinating encephalitis [2]. The prominent immunosuppression observed during disease progression is mainly mediated by viral blockade of the type-I interferon (IFN-α/β) signal transduction cascade, representing a key contributor to secondary infections and high case-fatality rates [3, 4].

Based on genetic and antigenic variations, CDV is classified into 17 genotypes. Three genotypes, namely Asia-1, Arctic-like and Asia-3, are currently circulating in China, among which Asia-1 is the predominant strain [5]. Notably, frequent CDV outbreaks have occurred in major mink-breeding regions of Shandong Province and other areas in China in recent years, characterized by acute onset, rapid transmission, and high lethality. The mortality rate in local farms has increased markedly compared with historical levels [6]. However, the underlying mechanisms responsible for this epidemiological change remain unclear, which is presumed to be associated with antigenic variation and virulence enhancement of prevailing CDV strains. Variant strains may evade host innate immune responses through amino acid mutations in key viral proteins, thereby acquiring enhanced pathogenicity. Previous whole-genome sequencing analysis of currently prevalent CDV strains conducted by our research group revealed that newly isolated strains share high homology with each other (98.4%–99.6%), whereas they exhibit relatively low genetic relatedness to historical reference strains (97.4%–98.9%) and form an independent clade in the phylogenetic tree. Of particular note, all recently isolated strains carry two fixed mutations, I542N and Y549H, within the receptor-binding site (RBS) of the hemagglutinin (H) protein. Regular amino-acid variations were also identified in proteins involved in viral genomic RNA synthesis. These observations suggest that genome-wide mutations may be closely linked to the increased pathogenicity of these strains.

## 2. Materials and methods

# 2.1 Experimental Animals and Viruses

Sixty-day-old purebred short-haired black minks (body weight: 0.6 kg–0.75 kg) used in this study were supplied by the Fur Animal Experimental Base of the Institute of Special Animal and Plant Sciences, Chinese Academy of Agricultural Sciences. All minks tested negative for CDV antigen and antibodies.

The SDZC(17)M2 (GenBank accession No. MK408454) and LNDL(17)M4 (GenBank accession No. MK408453) strains used in this study were isolated from CDV-diseased minks in Shandong and Liaoning provinces using the canine SLAM-expressing Vero cell line (Vero-cSLAM, VDS). The Hebei strain (GenBank accession No. KC427278.1) was isolated from CDV-infected minks in Hebei Province with conventional Vero cells. The H-protein mutation profiles of the three strains were characterized as follows: SDZC(17)M2 harbored double amino-acid mutations I542N/Y549H in the H protein;

LNDL(17)M4 possessed a single Y549H mutation in the H protein; no mutations at these positions were detected in the Hebei strain. The viral titers of Hebei, LNDL(17)M4 and SDZC(17)M2 were $10^{4.5}$, $10^{4.5}$ and $10^{5.33}$ $TCID_{50}$/mL, respectively.

## 2.2 Virus Challenge and Sample Collection in Minks

Sixty-day-old minks were randomly allocated into four groups (five animals per group). Three groups were intranasally challenged with the Hebei, LNDL(17)M4 and SDZC(17)M2 strains, respectively, via 1 mL nasal inoculation at a viral titer of $10^{4.0}$ $TCID_{50}$/mL. The control group received 1 mL of DMEM intranasally. All animals were raised under isolated conditions, and clinical signs including body temperature, body weight and fecal status were monitored daily.

Nasal and rectal swabs were collected from each mink on days 0, 3, 7, 10, 14 and 21 for viral load quantification. EDTA-anticoagulated whole blood and coagulated blood samples were harvested. Anticoagulated blood was used for hematological analysis and extraction of viral RNA, while serum separated from coagulated blood was stored at − 80°C for subsequent analyses. At 21 days post challenge, all minks were humanely euthanized under anesthesia and subjected to necropsy. Tissue samples including liver, spleen, lymph nodes, kidney, intestine and brain were collected for viral load detection, immunohistochemistry and histopathological examination.

## 2.3 Lymphocyte Counting and CDV Neutralizing Antibody Assay

Approximately 15 μL of EDTA-anticoagulated peripheral blood was collected from minks at different time points (days 0, 3, 7, 10, 14 and 21), and lymphocyte counts were determined using an automated hematology analyzer. For neutralizing antibody detection, serum samples were prepared as serial two-fold dilutions. The CDV neutralizing antibody titers against 100 $TCID_{50}$ of the SD(14)7 strain were measured on Vero-cSLAM cells following the protocol described by Stephensen et al. [7]. Neutralizing antibody titers were calculated using the Reed–Muench method [8].

## 2.4 Quantification of Viral RNA by Real-Time Quantitative PCR

Viral RNA was extracted from nasal-ocular and rectal swabs using the QIAamp Viral RNA Kit, from tissue samples using the RNeasy Mini Kit, and from EDTA-anticoagulated peripheral blood using the QIAamp Blood RNA Mini Kit. Purified viral RNA was reverse-transcribed into cDNA with random hexamer primers (N6) using the PrimeScript II 1st Strand cDNA Synthesis Kit according to the manufacturer's instructions. Real-time quantitative PCR (qPCR) was performed to quantify viral RNA loads in shedding samples and various animal tissues. The primer sequences, probe sequence and thermal cycling conditions for qPCR were adopted from Elia et al. [9].

Primer and probe sequences were listed as follows: Forward primer: 5' AGCTAGTTTCATCTTAACTATCAAATT 3'; Reverse primer: 5' TTAACTCTCCAGAAAACTCATGC 3'; Probe:

5'FAM-ACCCAAGAGCCGGATACATAGTTTCAATGC-TAMRA 3'. The probe was labeled with FAM reporter dye at the 5' end and TAMRA quencher at the 3' end. The total reaction volume was 20 μL, consisting of 10 μL Premix Ex Taq™ (Probe qPCR), 0.4 μL CDV-F (20 μM), 0.4 μL CDV-R (20 μM), 0.8 μL CDV-Pb, 2 μL cDNA template, and 6.4 μL nuclease-free double-distilled water. The thermal cycling protocol was set as: initial denaturation at 95°C for 30 s; followed by 45 cycles of denaturation at 95°C for 5 s, annealing at 60°C for 1 min, extension at 40°C for 30 s.

## 2.5 Pathological Observation and Immunohistochemistry

Necropsy was performed on deceased minks and minks euthanized at day 21 post-challenge (anesthetized and sacrificed with Zoletil at a dose of 10 mg per kilogram body weight). Clinical signs of each mink were observed and recorded. Tissue samples including lung, spleen, kidney, lymph nodes and brain were collected and fixed in 10% formalin solution. The samples were submitted to Jilin Yixiang Technology Co., Ltd. for hematoxylin-eosin (HE) staining and immunohistochemical assays.

## 2.6 Establishment and Scoring of Virulence and Immunosuppression Parameters

The evaluation system for CDV virulence and immunosuppression was adapted from Zhao [10] with minor modifications. Virulence indicators included fever, conjunctivitis, fecal condition and pathological lesions. Immunosuppression indicators consisted of lymphocyte count, viremia and neutralizing antibody level. Each indicator was scored on a scale ranging from 0 to 3 (Supplementary Table 1). Fever was defined as a rectal temperature above 41 ℃ in minks. Scores for conjunctivitis and fecal status were assigned based on the maximum severity observed in each animal during the experiment. Lymphocyte count and viremia were scored using the data collected at day 10 post-infection. Pathological lesions were evaluated from lung histopathological sections, and neutralizing antibody scoring used the peak antibody titer.

## 2.7 Semi-quantitative Detection of Cytokine mRNA

Approximately 200 μL of EDTA-anticoagulated peripheral blood collected from minks at different sampling time points was used for total RNA extraction with the QIAamp Blood RNA Mini Kit. A total of 100 ng RNA was reverse-transcribed into first-strand cDNA using Oligo (dT18) as the primer and the PrimeScript II 1st Strand cDNA Kit following the manufacturer's protocol. SYBR Green I-based real-time quantitative PCR (qPCR) was performed on a LightCycler96 instrument. The 20 μL reaction mixture contained 10 μL TB Green Fast qPCR Mix, 0.8 μL CDV-F (20 μM), 0.8 μL CDV-R (20 μM), 2 μL cDNA template, and 6.4 μL nuclease-free double-distilled water. The thermal cycling program was set as follows: initial denaturation at 94°C for 30 s; 40 cycles of 94°C for 5 s and 60°C for 10 s. Primer sequences for target and reference genes applied in this assay were adopted from Rolland-Turner et al. [11], as listed in Supplementary Table 2. Each sample was tested in three technical replicates. Relative gene expression levels were calculated using the $2^{-\Delta\Delta CT}$ method [12].

## 2.8 Statistical Analysis

GraphPad Prism 5.00 software was used for data visualization, and SPSS Statistics 17.0 software was applied for statistical analyses. One-way analysis of variance (ANOVA) was adopted for group comparisons. Differences were considered statistically significant at $P < 0.05$ (*), highly significant at $P < 0.01$ (**), and extremely significant at $P < 0.001$ (***).

## 3. Result

# 3.1 Clinical Manifestations in Infected Minks

Twenty minks were randomly divided into four groups. Minks in the three challenge groups were intranasally inoculated with 1 mL CDV suspensions of the Hebei, LNDL(17)M4, and SDZC(17)M2 strains at a titer of $10^{4.0}$ $TCID_{50}$, respectively; the control group received 1 mL of DMEM via the same route. Clinical signs were monitored throughout the trial. In the SDZC(17)M2 group, two minks died on day 8 and another two died on day 20 post-challenge, resulting in four deaths within 21 days and a mortality rate of 80% (4/5). Fatally infected minks exhibited typical clinical signs of canine distemper, including hyperthermia, conjunctivitis, diarrhea, and footpad hyperkeratosis. One mink in the Hebei group died on day 9 post-challenge, corresponding to a mortality rate of 20% (1/5), and this animal also displayed typical distemper symptoms. All five minks in the LNDL(17)M4 group survived until the end of the 21-day trial (5/5) (Fig. 1A,B). Rectal temperatures of all minks were continuously monitored from day 0 to day 21. Transient hyperthermia (temperature > 41 ℃, lasting 1–2 days) was observed in four minks of the SDZC(17)M2 group. One mink in the Hebei group developed short-term fever on day 7, whereas no febrile responses were detected in the LNDL(17)M4 group. No clinical signs of canine distemper, including fever, were observed in the control group throughout the trial (Fig. 1C).

# 3.2 Analysis of Immunosuppression Levels

CDV primarily damages immune organs and immune-related cells in minks, impairing the defensive function of the immune system and resulting in immunosuppression. EDTA-anticoagulated blood and coagulated blood samples were collected at sequential time points. Dynamic changes in lymphocyte counts, viremia, and neutralizing antibody titers were monitored to evaluate differences in immunosuppression induced by the three CDV strains.

For lymphocyte dynamics: lymphocyte counts in all challenge groups were approximately 5,000 cells/μL on day 0 post-challenge. On day 3, lymphocyte counts decreased to 2,100 cells/μL in the Hebei group, 1,700 cells/μL in the LNDL(17)M4 group, and 1,100 cells/μL in the SDZC(17)M2 group. Moreover, the lymphocyte count of the SDZC(17)M2 group reached 766 cells/μL on day 7, which was significantly lower than 2,000 cells/μL observed in the LNDL(17)M4 group ($P < 0.05$). On day 14, the lymphocyte count of the SDZC(17)M2 group (800 cells/μL) was significantly lower than that of the Hebei group (2,066 cells/μL) ($P < 0.05$). Overall, circulating lymphocyte counts in the SDZC(17)M2 group were lower than those in the Hebei and LNDL(17)M4 groups at days 3, 7, 10, 14 and 21 post-challenge. Lymphocyte counts remained around 5,000 cells/μL throughout the trial in the control group (Fig. 2A).

Quantitative real-time PCR was performed to detect viral RNA loads in peripheral blood. The results demonstrated that all three CDV strains replicated rapidly in minks and triggered viremia of varying severity. Viral RNA loads in peripheral blood rose quickly after challenge. No significant differences in viral RNA loads were observed between the Hebei group and LNDL(17)M4 group at days 3, 7, 10, 14 and 21 ($P > 0.05$), with peak loads up to 107 copies/mL. In contrast, viral RNA loads in the SDZC(17)M2 group were significantly higher than those in the Hebei and LNDL(17)M4 groups at days 7, 10, 14 and 21 ($P < 0.01$), reaching a maximum of $10^{11}$ copies/mL. No viral RNA was detected in samples from the control group (Fig. 2B).

A virus neutralization assay using 100 $TCID_{50}$ of the SD(14)7 strain was applied to measure neutralizing antibody levels in minks of the Hebei, LNDL(17)M4 and SDZC(17)M2 groups at different sampling time points. Neutralizing antibodies were detectable in all three groups starting at day 14, and peak titers ranging from 1:8 to 1:32 were achieved by day 21. Nevertheless, neutralizing antibody magnitudes remained low in all groups. Collectively, neutralizing antibody levels in the SDZC(17)M2 group were lower than those in the other two groups (Fig. 2C).

# 3.3 Histopathological and Immunohistochemical Results

## 3.3.1 Histopathology of Lung and Spleen Tissues

Histopathological observation and comparison of lung and spleen tissues from minks infected with different CDV strains revealed varying degrees of lesions induced by the three isolates. Widespread alveolar collapse, thickened alveolar walls and pulmonary consolidation were observed in the lungs of minks from the Hebei, LNDL(17)M4 and SDZC(17)M2 groups (Fig. 3a, 3b and 3c). Lesions were most severe in the SDZC(17)M2 group, where extensive destruction of pulmonary architecture and inflammatory cell infiltration were evident (Panel c, green arrows).

Spleen lesions included congestion and hemorrhage within splenic lymphoid sinuses, connective tissue hyperplasia in the intima of small blood vessels, parenchymal cell degeneration and necrosis, infiltration of macrophages and neutrophils, and markedly reduced lymphocyte populations. Splenic sinus congestion and splenomegaly were observed in all three challenge groups (Fig. 3d, 3e, 3f). Severe lymph sinus congestion and splenomegaly were observed in the Hebei and SDZC(17)M2 groups (Fig. 3d, 3f).

a: Histopathological changes in lung tissue of mink infected with Hebei strain; b: Histopathological changes in lung tissue of mink infected with LNDL(17)M4 strain; c: Histopathological changes in lung tissue of mink infected with SDZC(17)M2 strain; d: Histopathological changes in spleen tissue of mink infected with Hebei strain; e: Histopathological changes in spleen tissue of mink infected with LNDL(17)M4 strain; f: Histopathological changes in spleen tissue of mink infected with SDZC(17)M2 strain

## 3.3.2 Immunohistochemistry

Immunohistochemical staining targeting the CDV-N protein revealed positive CDV antigen signals in bronchial epithelial cells within the lungs of minks infected with the Hebei, LNDL(17)M4, and SDZC(17)M2 strains (Fig. 4a–c). Notably, the abundance of CDV antigen-positive signals in lung tissues was markedly higher in the SDZC(17)M2 group compared with the Hebei and LNDL(17)M4 groups. CDV antigen was detected in splenic lymphocytes from minks in the Hebei group (Fig. 4d). Only a small number of antigen-positive lymphocytes were observed in the LNDL(17)M4 group (Fig. 4e), whereas abundant CDV antigen-positive lymphocytes were identified in the SDZC(17)M2 group (Fig. 4f).

a–c: Immunohistochemical staining of lung tissues from minks infected with Hebei strain, LNDL(17)M4 strain and SDZC(17)M2 strain, respectively; d–f: Immunohistochemical staining of spleen tissues from minks infected with Hebei strain, LNDL(17)M4 strain and SDZC(17)M2 strain, respectively.

## 3.4 Viral Loads in Mink Tissues

Quantitative real-time PCR was used to detect the distribution of viral RNA loads in ocular-nasal swabs, rectal swabs and various tissue samples collected from minks infected with the three CDV strains. Viral RNA was detectable in ocular-nasal and rectal swabs of challenged minks starting at day 7 post-challenge. Viral RNA loads in rectal swabs of all three challenge groups peaked on day 10 post-challenge, reaching up to $10^9$ copies/mL, while peak viral loads in ocular-nasal swabs reached $10^8$ copies/mL. High viral RNA loads persisted from day 10 to day 14 (Fig. 5A). Viral RNA was still detectable in ocular-nasal and rectal swabs from all challenged minks at the end of the 21-day trial. Viral RNA loads in rectal swabs of the SDZC(17)M2 group were significantly higher than those in the Hebei and LNDL(17)M4 groups at days 10 and 14 ($P < 0.05$). On day 14, viral RNA loads in ocular-nasal swabs of the SDZC(17)M2 group were also significantly higher than those in the other two groups ($P < 0.05$). No significant differences in the mean viral RNA loads of rectal and ocular-nasal swabs were observed between the Hebei and LNDL(17)M4 groups at days 3, 7, 10, 14 and 21 (Fig. 5B). No viral RNA was detected in rectal or ocular-nasal swabs from all challenge groups at day 0 post-challenge, and only trace amounts of viral RNA were detected at day 3. No viral RNA was detected in negative control minks throughout the experiment.

The tissue distribution analysis revealed viral RNA in the liver, lung, lymph nodes, spleen, kidney and intestine. In the SDZC(17)M2 group, peak viral RNA loads in the lung, lymph nodes and kidney reached $10^9$ copies/mL, which were significantly higher than the corresponding tissue viral loads in the Hebei and LNDL(17)M4 groups ($P < 0.05$). Viral loads in the lung, lymph nodes and kidney of the Hebei group were slightly higher than those of the LNDL(17)M4 group. No significant intergroup differences in viral RNA loads in the liver, spleen and intestine were observed among all challenge groups ($P > 0.05$) (Fig. 5C). In addition, brain tissues were also examined, yet no viral RNA was detected in brain samples from any of the three challenge groups.

## 3.5 Pathogenicity Scoring of Different CDV Strains in Mink

Scores of virulence and immunosuppression were calculated according to the established evaluation system. The virulence score of the Hebei strain in minks was 1.1, the LNDL(17)M4 strain was 0.85, and the SDZC(17)M2 strain was 2. For immunosuppression scores, the Hebei strain was 2, the LNDL(17)M4 strain was 1.73, and the SDZC(17)M2 strain was 2.67. These data demonstrated that the SDZC(17)M2 strain exhibited the highest virulence and induced the strongest immunosuppression in minks, followed by the Hebei and LNDL(17)M4 strains (Table 1).

## 3.6 Alterations of Cytokine mRNA Expression in Minks Induced by CDV

SYBR Green I-based real-time quantitative PCR was performed to evaluate transcriptional changes in cytokine responses triggered by the Hebei, LNDL(17)M4, and SDZC(17)M2 strains. In minks infected with the three CDV strains, the mRNA transcription level of TNF-α decreased from day 3 to day 10 post-challenge, returned to baseline at day 14, and was downregulated again at day 21. The mRNA levels of IFN-α and IFN-β remained relatively unchanged from day 3 to day 10, followed by upregulation at day 14. The mRNA expression of IL-4 was continuously downregulated from day 3 to day 21 in all challenge groups. No statistically significant intergroup differences in the mRNA transcription levels of TNF-α, IFN-α, IFN-β and IL-4 were observed among the three challenge g

# 4.Discussion

CDV is a globally important pathogen of carnivores and causes severe pathogenicity and high mortality in farmed minks [13]. In recent years, frequent CDV outbreaks in major fur-breeding regions of China, including Shandong, Hebei, and Liaoning provinces, have resulted in considerable economic losses to the fur industry [13]. In the present study, three field CDV strains carrying distinct mutations in the hemagglutinin (H) protein were isolated from these epidemic regions and used for artificial infection in minks. The present study systematically compared the pathogenicity, immunosuppressive potential, and tissue tropism of the three strains, aiming to elucidate the relationship between H-protein mutations and the heterogeneous virulence of different CDV field isolates.

As the major receptor-binding envelope protein of CDV, the H protein plays a pivotal role in viral adsorption, host cell entry, and the induction of neutralizing antibody responses [14, 15]. Amino acid mutations at specific sites within the H gene can markedly alter viral binding affinity for host receptors, thereby modifying the host range, tissue tropism, and pathogenic characteristics of CDV [15, 16]. In the present study, the three epidemic CDV strains harbored distinct sets of mutations in the H protein. The SDZC(17)M2 (Shandong) strain carried dual mutations I542N and Y549H; the LNDL(17)M4 (Liaoning) strain possessed only the single Y549H mutation, whereas the Hebei strain lacked mutations at these key sites [5]. In vivo infection results demonstrated that the SDZC(17)M2 strain induced the highest mortality, the most severe clinical signs, and the most extensive histopathological lesions, accompanied by the highest viral loads across multiple tissues. The Hebei strain exhibited moderate pathogenicity, while LNDL(17)M4 displayed the weakest virulence. These findings are consistent with a previous report

describing the dual-mutant strain SD(14)7 carrying identical I542N/Y549H substitutions, which showed greater virulence and immunosuppressive effects than wild-type CDV [10]. Collectively, these results indicate that the I542N and Y549H mutations in the H protein are closely associated with enhanced virulence and strengthened immunosuppressive potential of circulating CDV strains in minks.

Notably, the I542N mutation in the H protein of the SDZC(17)M2 strain creates a novel potential N-linked glycosylation site spanning amino acid residues 542–544 [6]. As a heavily glycosylated membrane protein, the CDV H protein relies strongly on N-linked glycosylation for proper expression, folding, intracellular trafficking and biological function [17]. Previous studies have demonstrated that additional N-glycosylation sites can enhance viral virulence, while removal of specific N-glycosylation sites within the CDV H protein markedly attenuates viral pathogenicity in ferrets [17]. Therefore, the extra glycosylation site introduced by the I542N mutation in SDZC(17)M2 may alter the spatial conformation and receptor-binding affinity of the H protein, thereby increasing viral replication efficiency in vivo. This structural change likely constitutes one key molecular mechanism contributing to the enhanced pathogenicity of this Shandong isolate. Moreover, the Y549H mutation has previously been reported to increase CDV pathogenicity and immunosuppressive potential in ferrets [15]. Substitution of residue 549 between tyrosine (feline-adapted) and histidine (canine-adapted) markedly increases membrane fusion efficiency and viral titers of canine-origin CDV in feline cells [18], demonstrating that Y549H plays a critical role in host adaptation and cross-species transmission. In the present study, the single Y549H-mutant LNDL(17)M4 strain exhibited weaker pathogenicity than the non-mutated Hebei strain, and no significant intergroup differences in virulence or immunosuppression were detected between these two strains. These findings indicate that the Y549H single mutation alone is insufficient to significantly enhance CDV virulence in minks.

It is noteworthy that SDZC(17)M2 carrying dual I542N/Y549H mutations exhibited markedly higher pathogenicity than LNDL(17)M4 carrying the single Y549H mutation and the non-mutated Hebei strain. This observation suggests that I542N and Y549H may exert synergistic effects rather than functioning independently. The three-dimensional structural model of CDV H protein in complex with its SLAM receptor indicates that residues 542 and 549 are both located within the receptor-binding site (RBS) of the H protein. Furthermore, amino acids at positions 542 and 549 of CDV H protein are predicted to interact with residue 126 of the SLAM receptor [13]. The spatial proximity of these two mutation sites within the RBS may provide a potential structural basis for such synergistic interactions. The I542N mutation may not only improve protein stability or receptor affinity via the introduction of an additional N-linked glycosylation site, but also alter the conformational and electrostatic properties of the amino acid side chain at residue 542. Such changes could further modulate the interaction between the adjacent residue 549 and residue 126 of the SLAM receptor, which may in turn contribute to enhanced binding efficiency between the H protein and its receptor. This hypothesis of spatial synergism between these two sites aligns with the findings from von Messling et al. [15], who demonstrated that multiple amino acid substitutions within the RBS of morbillivirus H protein can synergistically modulate viral virulence.

To further evaluate the differential host immune responses induced by distinct CDV strains, the mRNA transcription levels of TNF-α, IFN-α, IFN-β and IL-4 in peripheral blood were determined in the present study. The results indicated that CDV infection induced marked disturbance of cytokine expression. The pro-inflammatory TNF-α was downregulated during the early infection stage, the antiviral IFN-α and IFN-β were significantly upregulated at day 14, and the Th2-type IL-4 was continuously downregulated throughout the infection period. Despite the distinct pathogenic phenotypes among the three strains, no significant intergroup differences in cytokine transcription levels were observed. The early suppression of TNF-α and the late activation of IFN-α/β suggest that CDV may weaken the host's early antiviral defense by inhibiting pro-inflammatory responses, while the interferon pathway may be activated in response to persistent viral replication pressure. Moreover, the sustained downregulation of IL-4 indicates that CDV infection may disrupt the Th1/Th2 immune balance, a finding consistent with a Th1-biased immune response.

Notably, although the cytokine transcription patterns induced by the three strains were similar, the SDZC(17)M2 group exhibited markedly higher viral loads and a more severe immunosuppressive phenotype. This result suggests that the highly virulent SDZC(17)M2 strain, owing to its stronger in vivo replication capacity, may elicit sustained and intense antigenic stimulation, potentially aggravating immune cell loss and functional impairment. Even though no significant intergroup differences in cytokine transcription levels were detected, the substantial reduction in lymphocyte numbers caused by SDZC(17)M2 infection likely impaired the overall immune reserve and antiviral defense capacity of the host, which may contribute to the more severe immunosuppression and tissue damage observed in this group.

# 5.Conclusion

The three CDV strains induced clinical signs of varying severity and multisystemic pathological organ lesions in minks. The mortality rates for the SDZC(17)M2, Hebei, and LNDL(17)M4 groups were 80%, 20%, and 0, respectively. Distinct virulence and immunosuppression levels were observed among animals infected with the three isolates. The virulence-to-immunosuppression scores for SDZC(17)M2, Hebei, and LNDL(17)M4 were 2/2.67, 1.1/2, and 0.85/1.73, correspondingly. All three strains replicated robustly in vivo. The SDZC(17)M2 group exhibited the highest viral RNA loads up to $10^9$ copies/mL in lungs, lymph nodes and kidneys, which were significantly higher than those of the Hebei and LNDL(17)M4 groups. Moreover, viral RNA loads in nasal-ocular and rectal swabs collected at day 14 post-infection were markedly higher in the SDZC(17)M2 group relative to the other two groups.

# Declarations

### Ethics statement

All animal experiments were carried out following the national guidelines for the care and use of laboratory animals and the ARRIVE guidelines. All experimental procedures were reviewed and approved

by the Animal Ethics Committee of Guizhou Medical University (No. 2100216). All efforts were made to minimize animal suffering.

**Author contributions**

Rong-Shan Tao, Dingfeng Long (Co-first authors): Conceptualization, Methodology, Formal analysis, Software, Data curation, Visualization, Writing – original draft.

Jianjun Zhao*, Yu Cao* (Corresponding authors): Conceptualization, Resources, Supervision, Funding acquisition, Writing – review & editing.

**Funding**

The author(s) declare that financial support was received for the research and/or publication of this article. This work was supported by the Guizhou Provincial Basic Research Program (Natural Science) (Grant Nos. qkhjc-ZK [2024]134), the Guizhou Provincial Basic Research Program (Natural Science) (Grant Nos. qkhjc-MS [2026]537), the Technology Fund Project of Guizhou Provincial Health Commission (Grant Nos. gzwkj2025-533), the Guizhou Health Development Research Institute (Guizhou Medical University) (No. KP2026013)College Students Innovation and Entrepreneurship Training Program of Guizhou Province (Grant Nos. S202310660092, S2024106601375, S202510660239S202610660336).

## Conflict of interest

## All authors declare no financial or personal relationships with other people or organizations that could inappropriately influence their work. No potential conflict of interest was reported.

# References

1. Kapil S, Allison RW, Johnston L 3rd, Murray BL, Holland S, Meinkoth J et al (2008) Canine distemper virus strains circulating among North American dogs. Clin Vaccine Immunol 15(4):707–712. https://doi.org/10.1128/cvi.00005-08
2. Visser IK, Vedder EJ, van de Bildt MW, Orvell C, Barrett T, Osterhaus AD (1992) Canine distemper virus ISCOMs induce protection in harbour seals (Phoca vitulina) against phocid distemper but still allow subsequent infection with phocid distemper virus-1. Vaccine 10(7):435–438. https://doi.org/10.1016/0264-410x(92)90390-6
3. von Messling V, Milosevic D, Cattaneo R (2004) Tropism illuminated: lymphocyte-based pathways blazed by lethal morbillivirus through the host immune system. Proc Natl Acad Sci U S A 101(39):14216–14221. https://doi.org/10.1073/pnas.0403597101
4. von Messling V, Svitek N, Cattaneo R (2006) Receptor (SLAM [CD150]) recognition and the V protein sustain swift lymphocyte-based invasion of mucosal tissue and lymphatic organs by a morbillivirus. J Virol 80(12):6084–6092. https://doi.org/10.1128/jvi.00357-06

5. Tao R, Chen J, Zhao T, Gong C, Pan H, Akhtar RW et al (2020) Comparison of Growth Characteristics and Genomics of Two Canine Distemper Virus Strains Isolated From Minks in China. Front Vet Sci 7:570277. https://doi.org/10.3389/fvets.2020.570277
6. Zhao J, Zhang H, Bai X, Martella V, Hu B, Sun Y et al (2014) Emergence of canine distemper virus strains with two amino acid substitutions in the haemagglutinin protein, detected from vaccinated carnivores in North-Eastern China in 2012–2013. Vet J 200(1):191–194. https://doi.org/10.1016/j.tvjl.2014.01.028
7. Stephensen CB, Welter J, Thaker SR, Taylor J, Tartaglia J, Paoletti E (1997) Canine distemper virus (CDV) infection of ferrets as a model for testing Morbillivirus vaccine strategies: NYVAC- and ALVAC-based CDV recombinants protect against symptomatic infection. J Virol 71(2):1506–1513. https://doi.org/10.1128/jvi.71.2.1506-1513.1997
8. REED LJ, MUENCH H, A SIMPLE METHOD OF ESTIMATING FIFTY PER CENT ENDPOINTS (1938). American Journal of Epidemiology 27(3):493–497. https://doi.org/10.1093/oxfordjournals.aje.a118408%J American Journal of Epidemiology
9. Elia G, Decaro N, Martella V, Cirone F, Lucente MS, Lorusso E et al (2006) Detection of canine distemper virus in dogs by real-time RT-PCR. J Virol Methods 136(1):171–176. https://doi.org/https://doi.org/10.1016/j.jviromet.2006.05.004
10. Zhao J, Shi N, Sun Y, Martella V, Nikolin V, Zhu C et al (2015) Pathogenesis of canine distemper virus in experimentally infected raccoon dogs, foxes, and minks. Antiviral Res 122:1–11. https://doi.org/10.1016/j.antiviral.2015.07.007
11. Rolland-Turner M, Farré G, Boué F (2006) Cloning of fox (Vulpes vulpes) Il2, Il6, Il10 and IFNγ and analysis of their expression by quantitative RT-PCR in fox PBMC after in vitro stimulation by Concanavalin A. Vet Immunol Immunopathol 110(3):369–375. https://doi.org/https://doi.org/10.1016/j.vetimm.2005.10.006
12. Schmittgen TD, Zakrajsek BA, Mills AG, Gorn V, Singer MJ, Reed MW (2000) Quantitative Reverse Transcription–Polymerase Chain Reaction to Study mRNA Decay: Comparison of Endpoint and Real-Time Methods. Anal Biochem 285(2):194–204. https://doi.org/https://doi.org/10.1006/abio.2000.4753
13. Tao R, Ba H, Chen J, Liu M, Pan H, Li X et al (2020) Phylodynamic analysis of two amino acid substitutions in the hemagglutinin protein of canine distemper virus strains detected in fur-bearing animals in China. Virus Genes 56(1):58–66. https://doi.org/10.1007/s11262-019-01720-9
14. Sato H, Yoneda M, Honda T, Kai C (2012) Morbillivirus Receptors and Tropism: Multiple Pathways for Infection. 3–2012. https://doi.org/10.3389/fmicb.2012.00075
15. von Messling V, Springfeld C, Devaux P, Cattaneo R (2003) A ferret model of canine distemper virus virulence and immunosuppression. J Virol 77(23):12579–12591. https://doi.org/10.1128/jvi.77.23.12579-12591.2003
16. Zipperle L, Langedijk JPM, Örvell C, Vandevelde M, Zurbriggen A, Plattet P (2010) Identification of Key Residues in Virulent Canine Distemper Virus Hemagglutinin That Control CD150/SLAM-Binding

Activity. 84(18):9618–9624. https://doi.org/doi:10.1128/jvi.01077-10

17. Sawatsky B, Messling V (2010) Canine Distemper Viruses Expressing a Hemagglutinin without N-Glycans Lose Virulence but Retain Immunosuppression. 84(6):2753–2761. https://doi.org/doi:10.1128/jvi.01813-09
18. Nikolin VM, Osterrieder K, von Messling V, Hofer H, Anderson D, Dubovi E et al (2012) Antagonistic pleiotropy and fitness trade-offs reveal specialist and generalist traits in strains of canine distemper virus. PLoS ONE 7(12):e50955. https://doi.org/10.1371/journal.pone.0050955

## Table 1

Table 1 is available in the Supplementary Files section.

## Figures

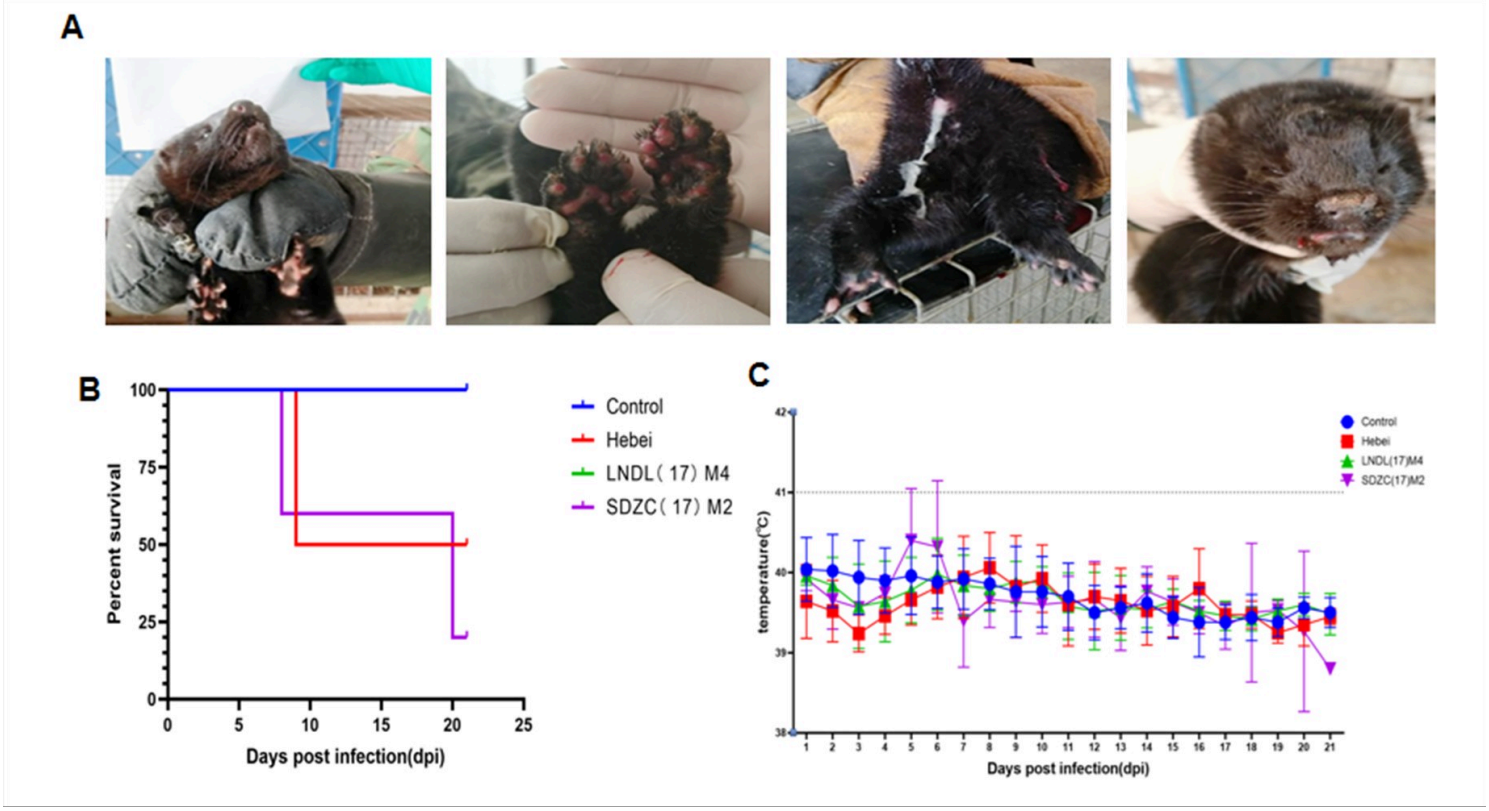
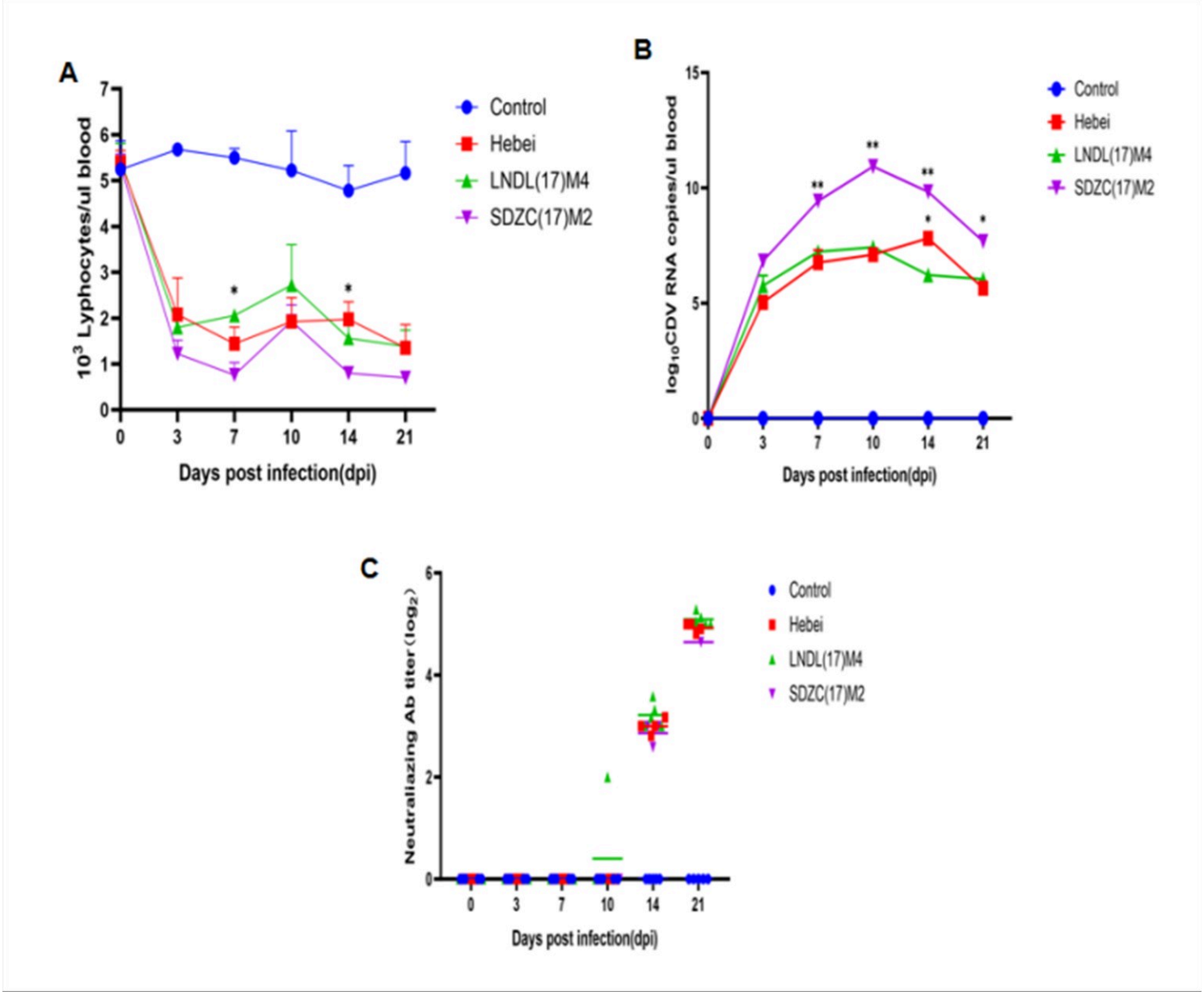



**Figure 1**

Clinical manifestations of minks infected with CDV. A. Clinical signs of CDV-infected minks; B. Survival curves of minks after CDV infection; C. Mean rectal temperature of minks. Clinical symptoms of CDV infection with mink (b, c, d) compared with negative control mink(a).




## Figure 2

Analysis of immunosuppression levels. A. Peripheral blood lymphocyte counts in minks following CDV challenge; B. Viral RNA loads in peripheral blood samples measured by quantitative real-time PCR; C. Detection of neutralizing antibodies after CDV challenge.

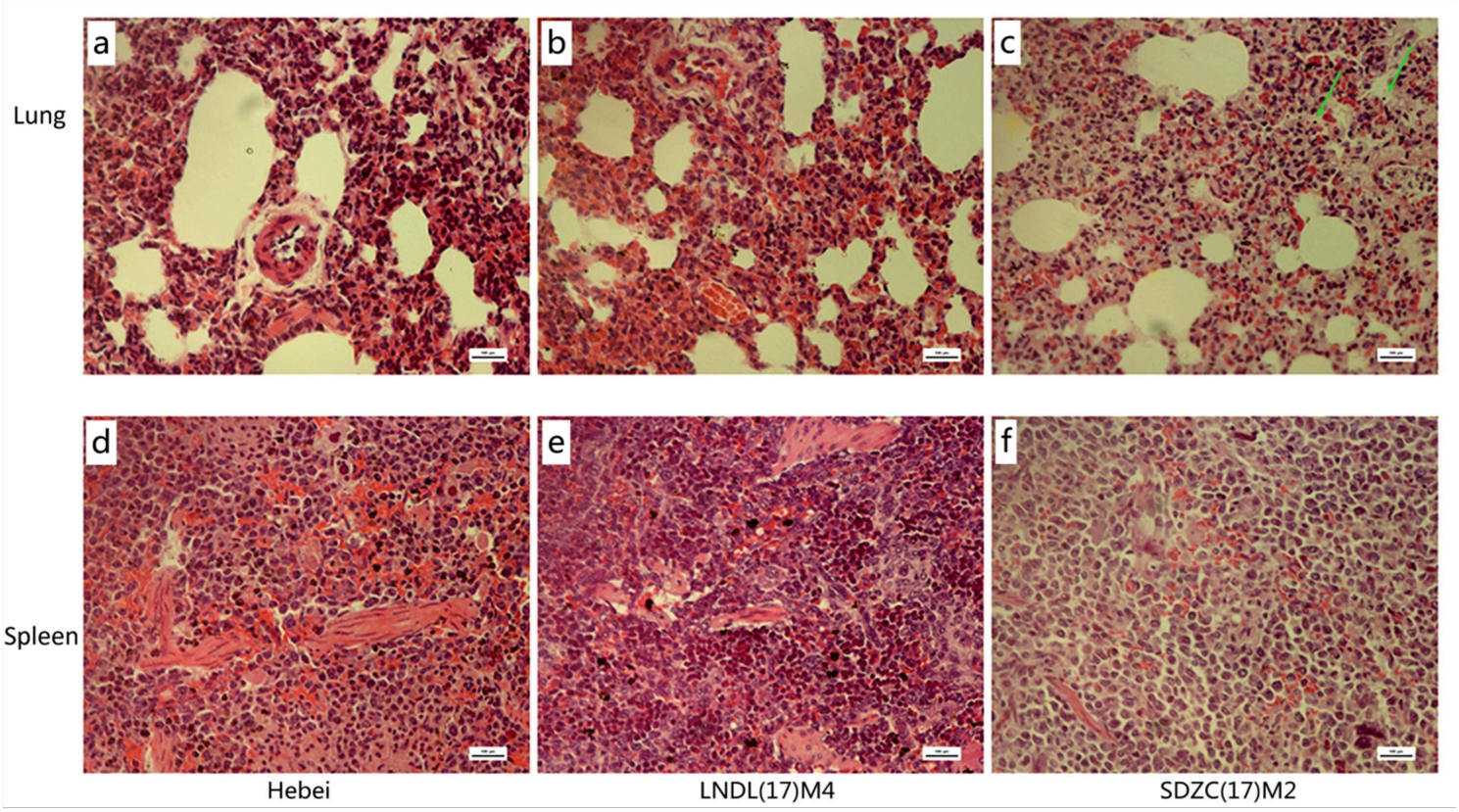



**Figure 3**

Histological sections of lungs and spleens from CDV-infected minks (×100)

a: Histopathological changes in lung tissue of mink infected with Hebei strain; b: Histopathological changes in lung tissue of mink infected with LNDL(17)M4 strain; c: Histopathological changes in lung tissue of mink infected with SDZC(17)M2 strain; d: Histopathological changes in spleen tissue of mink infected with Hebei strain; e: Histopathological changes in spleen tissue of mink infected with LNDL(17)M4 strain; f: Histopathological changes in spleen tissue of mink infected with SDZC(17)M2 strain

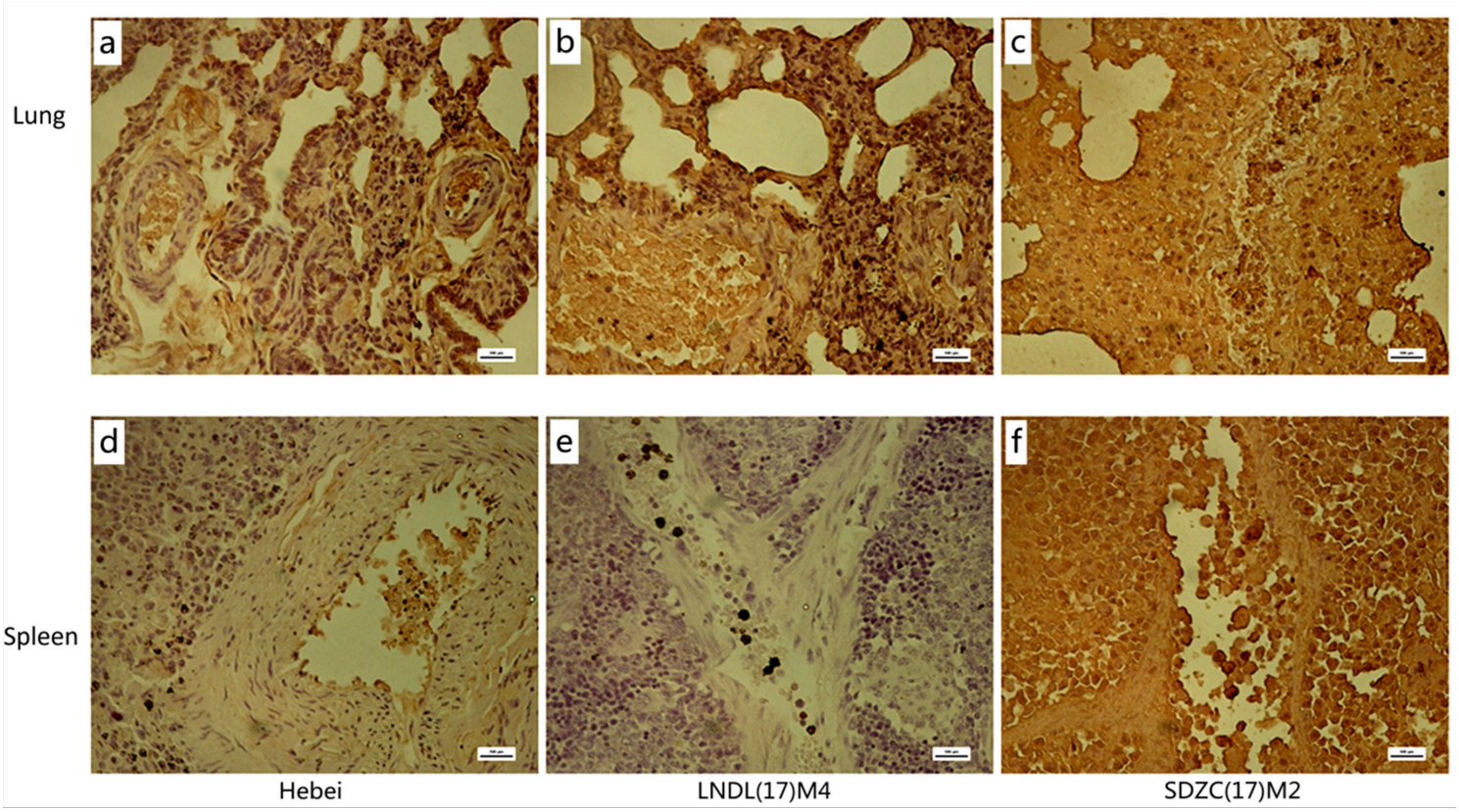
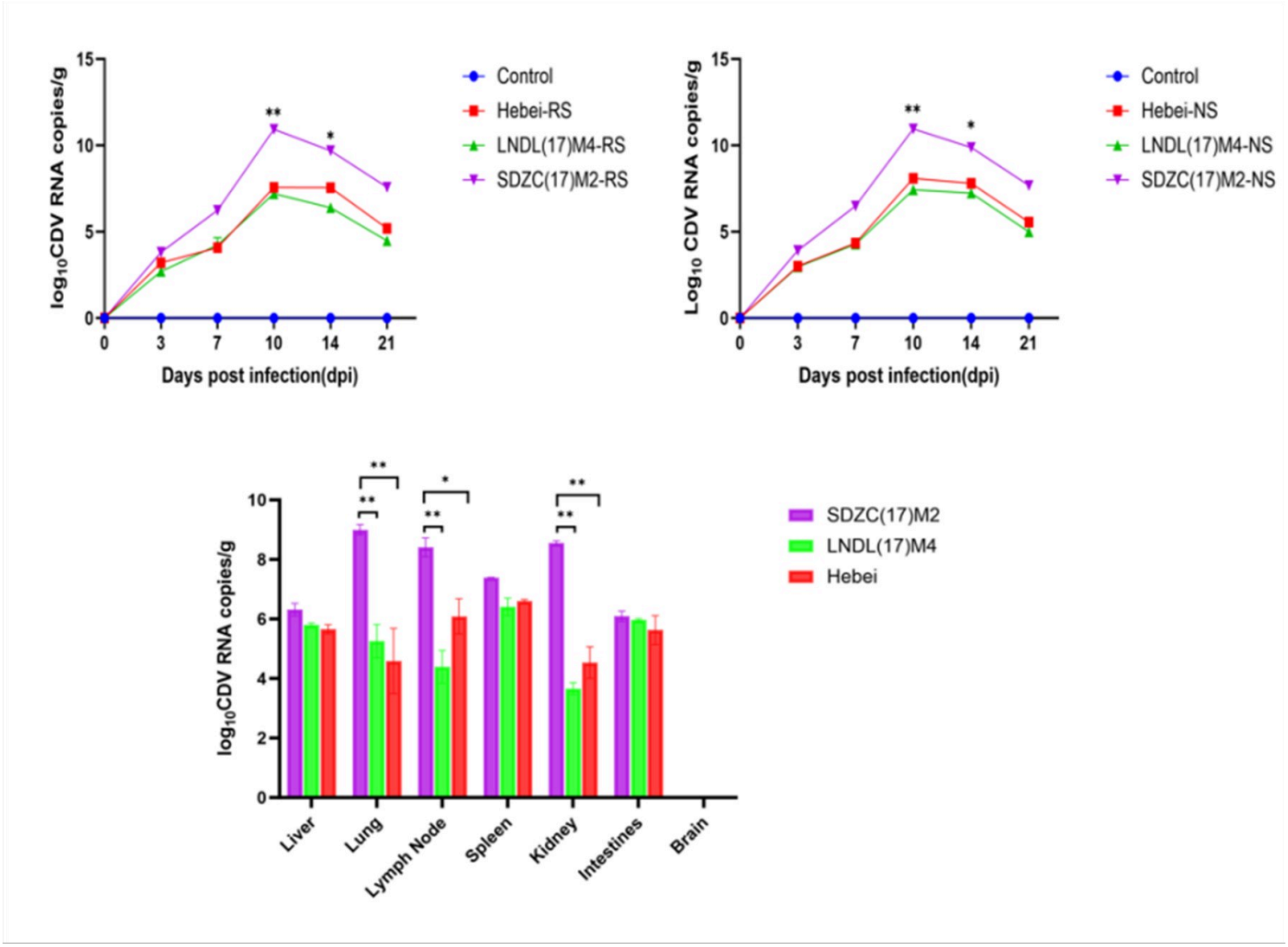



**Figure 4**

Immunohistochemistry of lungs and spleens from CDV-infected minks (×100)

a–c: Immunohistochemical staining of lung tissues from minks infected with Hebei strain, LNDL(17)M4 strain and SDZC(17)M2 strain, respectively; d–f: Immunohistochemical staining of spleen tissues from minks infected with Hebei strain, LNDL(17)M4 strain and SDZC(17)M2 strain, respectively.




## Figure 5

Viral RNA loads in rectal swabs (RS), ocular-nasal swabs (NS), and different tissues from CDV-infected minks. A. Viral RNA loads in rectal swabs; B. Viral RNA loads in ocular-nasal swabs; C. Viral RNA loads in different tissues.

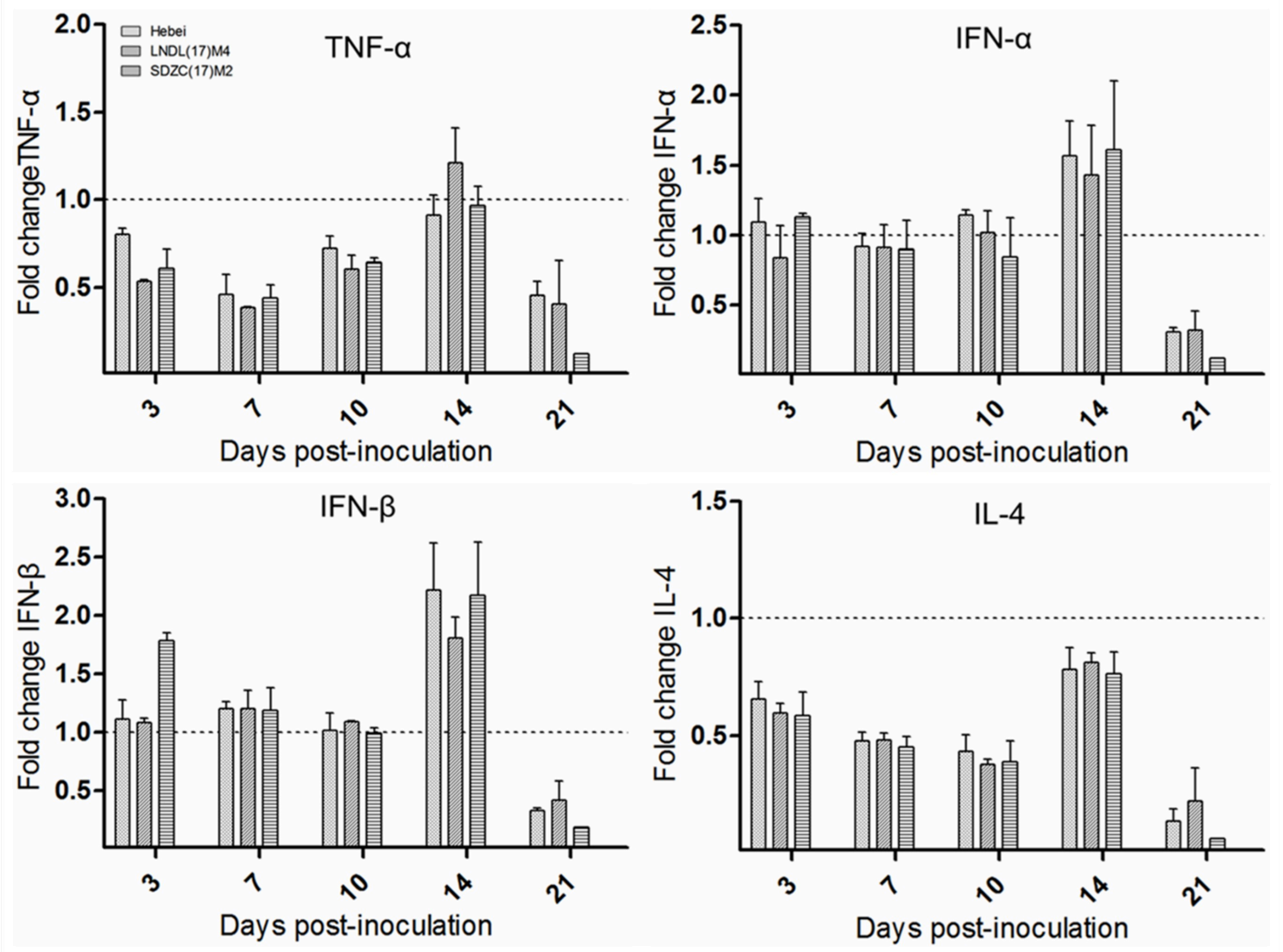



**Figure 6**

Comparison of mRNA transcription levels of TNF-α, IFN-α, IFN-β, and IL-4 in minks infected with CDV.

## Supplementary Files

This is a list of supplementary files associated with this preprint. Click to download.

- supplementaryMaterials.docx
- Table1.docx